YUKAWA-UNIFIED SUSY AND 7 TEV LHC

S. KRAML
Laboratoire de Physique de Subatomique et de Cosmologie (LPSC), UJF Grenoble 1, CNRS/IN2P3, INPG, 53 Avenue des Martyrs, F-38026 Grenoble, France

Simple SUSY GUT models based on the gauge group SO(10) require $t-b-\tau$ Yukawa coupling unification, in addition to gauge coupling and matter unification. The Yukawa coupling unification places strong constraints on the expected superparticle mass spectrum, with 1st/2nd generation scalar masses around 10 TeV while gluino masses are much lighter: in the 300500 GeV range. We hence expect large rates for gluino-pair production at hadron colliders, followed by decays to final states with large b-jet multiplicity. We discuss the discovery reaches for the Tevatron and the LHC at 7 TeV. We find that the early LHC reach for Yukawa-unified SUSY should be enough to either claim a discovery of the gluino, or to practically rule out this class of models.

1 Introduction

Grand unified theories (GUTs) find a welcome inclusion of supersymmetry (SUSY) into their structure in that SUSY tames the gauge hierarchy problem via the well-known cancellation of quadratic divergences [1]. In particular, the GUT group SO(10) is highly motivated in that it allows for– in addition to gauge unification– the unification of all the matter superfields of each generation into the 16-dimensional spinor representation [2]. The matter unification only works if the 15 matter superfields of the Minimal Supersymmetric Standard Model (MSSM) are augmented by a SM gauge singlet superfield $\hat{N}_i^c$ which contains a right-hand neutrino (RHN) field. The presence of RHN fields is essential to describe data from the past decade on neutrino mass and flavor oscillations; in particular a Majorana mass term near the GUT scale, needed to implement see-saw neutrino masses [3], should be generated by the breakdown of $SO(10)$ gauge symmetry. In addition to gauge and matter unification, in the simplest $SO(10)$ SUSY GUT models– wherein both MSSM Higgs doublets reside in a 10 of $SO(10)$– one expects *Yukawa coupling unification* in the third generation: $f_t = f_b = f_\tau$ $(= f_{\nu_\tau})$ at $M_{\rm GUT}$.

Recently, a variety of studies have examined the MSSM(+RHN) to check whether the measured values of gauge couplings and third generation fermion masses do indeed allow for $t-b-\tau$ Yukawa coupling unification [4–15]. Essential to the calculation is the inclusion of 2-loop renormalization group equations [16] (RGEs) and inclusion of weak scale threshold corrections [17] which occur due to the MSSM $\to$ SM transition in effective field theories. These threshold corrections imply that Yukawa coupling unification depends on the entire spectrum of SUSY particles, since the SUSY particles enter the various t, b and τ self-energy diagrams [17].

Assuming universal boundary conditions at the GUT scale, the parameter space of our $SO(10)$-motivated SUSY model consists of

$$m_{1/2},\ m_{16},\ m_{10},\ M_D^2,\ A_0,\ \tan\beta,\ sign(\mu), \tag{1}$$

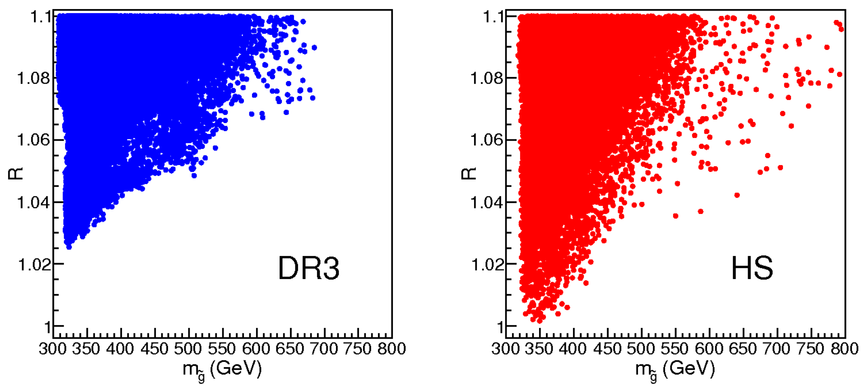

Figure 1: Scatter plot of Yukawa unified models in the R *vs.* $m_{\tilde{g}}$ plane, for solutions in the DR3 model (blue) and the HS model (red).

where $m_{1/2}$ is the common gaugino mass at $M_{\rm GUT}$, m_{16} is the common GUT mass of all matter scalars, m_{10} is that of the Higgs soft terms, and M_D^2 parametrizes potential splittings in the GUT scale Higgs (and possibly matter scalar) soft terms. Such splittings are expected to arise from the breaking of the $SO(10)$. It has been found that $t-b-\tau$ Yukawa coupling unification can occur in the MSSM within this setup, but only for very restricted forms of the soft SUSY breaking parameters at $M_{\rm GUT}$. For the case of $\mu>0$, preferred by BR($b\to s\gamma$), these are:

$$m_{16}\sim 5-15\ {\rm TeV},\ A_0\sim -2m_{16},\ m_{1/2}\ll m_{16},\ \tan\beta\sim 50. \tag{2}$$

These boundary conditions give rise to an inverted scalar mass hierarchy, wherein first/second generation scalars end up with masses ~ 10 TeV, while third generation scalars, Higgs scalars $A,\ H$ and $H^\pm$ and μ are of order $\sim 1-2$ TeV.[a]

To achieve radiative electroweak symmetry breaking (REWSB), the Higgs soft terms have to be split at $M_{\rm GUT}$, with $m_{H_u}^2 < m_{H_d}^2$, thus giving $m_{H_u}^2$ a head start over $m_{H_d}^2$ in its running towards the weak scale.[b] Such splitting naturally occurs due to D-term (DT) contributions to all scalar masses arising from the breakdown of $SO(10)$. Most studies however applied the splitting to only the Higgs sector ("just-so" Higgs splitting, HS)

$$m_{H_{u,d}}^2 = m_{10}^2 \mp 2M_D^2 \qquad \text{(HS model)} \tag{3}$$

because it results in better Yukawa unification as compared to full DT splitting. In [15] it has been shown that DT splitting, combined with the running effect of the neutrino Yukawa coupling f_{ν_τ} and a small mass splitting between first/second versus third generation scalars (the DR3 model) can allow for Yukawa coupling unification to a few percent.

Both the HS and DR3 schemes lead to mass spectra characterized by (i) 1st/2nd generation scalars with masses in the ~ 10 TeV range, (ii) third generation scalars in the ~ 1 TeV range, (iii) light gluinos with $m_{\tilde{g}}\sim 300-500$ GeV, (iv) a light bino-like LSP with $m_{\widetilde{Z}_1}\sim 50-90$ GeV. We quantify the degree of Yukawa unification as

$$R=\frac{max(f_t,\ f_b,\ f_\tau)}{min(f_t,\ f_b,\ f_\tau)} \tag{4}$$

where $f_t,\ f_b$ and f_τ are the top, bottom and tau Yukawa couplings, respectively, evaluated at $Q=M_{\rm GUT}$. Figure 1 shows the location of a large number of Yukawa-unified models in the

[a] Scenarios with very light H/A are excluded by BR($B_s\to\mu^+\mu^-$), see e.g. [11, 12, 15].

[b] This can be different in non-universal models, see [10, 13, 14].

R *vs.* $m_{\tilde{g}}$ plane, for the HS model (red dots) and the DR3 model (blue dots) obtained through a Markov Chain Monte Carlo (MCMC) scan of the parameter space (for details, see [15]). As can be seen, if we require $R < 1.05$ in the DR3 case, then $m_{\tilde{g}}$ is at most about 550 GeV. In the HS model, while $m_{\tilde{g}} \sim 300 - 500$ GeV is favored for low $R < 1.05$ solutions, it is possible (but not likely) to have scearios with $m_{\tilde{g}}$ as large as ~ 700 GeV.

Since the value of $m_{\tilde{g}}$ is so low in Yukawa-unified SUSY models, we expect the whole scenario to soon be tested at the CERN LHC [18] and to some extend also at the Fermilab Tevatron collider [19]. This is the main topic of this contribution.

Before we proceed to discuss collider phenomenology, two comments is in order First, under the assumption of gaugino mass unification, the LEP2 chargino mass limit that $m_{\widetilde{W}_1} > 103.5$ GeV normally implies that $m_{\tilde{g}} > 430$ GeV. However, in Yukawa-unified SUSY, the large trilinear soft breaking term $A_0 \sim -2m_{16}$ causes a large effect on gaugino mass evolution through two-loop RGE terms, resulting in a much smaller splitting between gaugino masses M_2 and M_3 than in mSUGRA-like cases. Thus gluino masses as low as ~ 300 GeV are possible respecting chargino mass bounds from LEP2.

THe second comments concerns the SUSY dark matter candidate. In models with the above listed superpartner spectrum and a bino-like $\widetilde{Z}_1$ state, the neutralino relic density is computed to be $\sim 10^2 - 10^4$ times the measured abundance [9,11] (unless one sits right on the h pole), and the models are seemingly excluded. However, if one invokes the Peccei-Quinn solution to the strong CP problem [20–24], then an axion/axino supermultiplet is expected in the theory [25]. With an axino of mass $m_{\tilde{a}} \sim 1$ MeV the neutralinos will decay via $\widetilde{Z}_1 \to \tilde{a}\gamma$, which greatly reduces the dark matter density by a large factor: $m_{\tilde{a}}/m_{\widetilde{Z}_1}$. Cold dark matter solutions can be found consisting of mainly cold axions and thermally produced axinos, with a small component of warm axinos arising from $\widetilde{Z}_1 \to \gamma\tilde{a}$ decay, which occurs on time scales of order 1 sec. Such scenarios are worked out in detail in [26].

2 Gluino cascade decays

Since $m_{\tilde{g}} \ll m_{\tilde{q}}$ in the HS and DR3 models, gluino decays are dominated by three-body modes. The branching ratios are in general largely model dependent, but since here $\tilde{t}_i$ and $\tilde{b}_i$ are always the lightest squarks, and $\tan\beta$ is large, the decays are mostly restricted to the following channels:

- $\tilde{g} \to \widetilde{Z}_i + b\bar{b}$, $i = 1, 2$
- $\tilde{g} \to \widetilde{Z}_1 + t\bar{t}$
- $\tilde{g} \to \widetilde{W}_1^- \bar{b}t$ or $\widetilde{W}_1^+ b\bar{t}$.

The general feature $m_{\tilde{g}} \ll m_{\tilde{q}}$ is common to both the HS and DR3 models, since it relies mostly on the fact that $m_{1/2} \ll m_{16}$. However, the inclusion of the D-term splitting for all matter scalars in the DR3 model pushes $m_{\tilde{b}_R}$ to lower values, when compared to the HS model, where $m_{\tilde{b}_L} \sim m_{\tilde{b}_R}$.[c] As a result we have $\tilde{b}_1 \sim \tilde{b}_R$ and $m_{\tilde{b}_1} < m_{\tilde{b}_2}$ in the DR3 case, while $\tilde{b}_1 \sim \tilde{b}_L$ and $m_{\tilde{b}_1} \sim m_{\tilde{b}_2}$ in the HS case. Now, since $\widetilde{Z}_2$ is wino-like in both models, it just couples to left-squarks, what suppresses the $\tilde{g} \to \widetilde{Z}_2 + b\bar{b}$ decay in the DR3 model and favors it in the HS case. Figure 2 shows typical branching fractions for model lines in the HS and DR3 schemes.

The $\widetilde{Z}_2$ and $\widetilde{W}_1$ also decay dominantly via three-body modes, $\widetilde{Z}_2 \to \widetilde{Z}_1 f\bar{f}$, $\widetilde{W}_1^\pm \to \widetilde{Z}_1 f\bar{f}'$, where the decays are primarily mediated by intermediate virtual W^* and Z^* diagrams (recall that the sleptons and squarks are very heavy). If $m_{\tilde{g}} \geq 500$ GeV, then the two-body modes $\widetilde{W}_1 \to \widetilde{Z}_1 W$ and $\widetilde{Z}_2 \to \widetilde{Z}_1 Z$ turn on.

[c] The stop masses and mixing are basically the same in both models, since the D-term splitting is equal for both $\tilde{t}_L$ and $\tilde{t}_R$, $m_Q^2 = m_U^2 = m_{16}^2 + M_D^2$, while $m_D^2 = m_{16}^2 - 3M_D^2$.

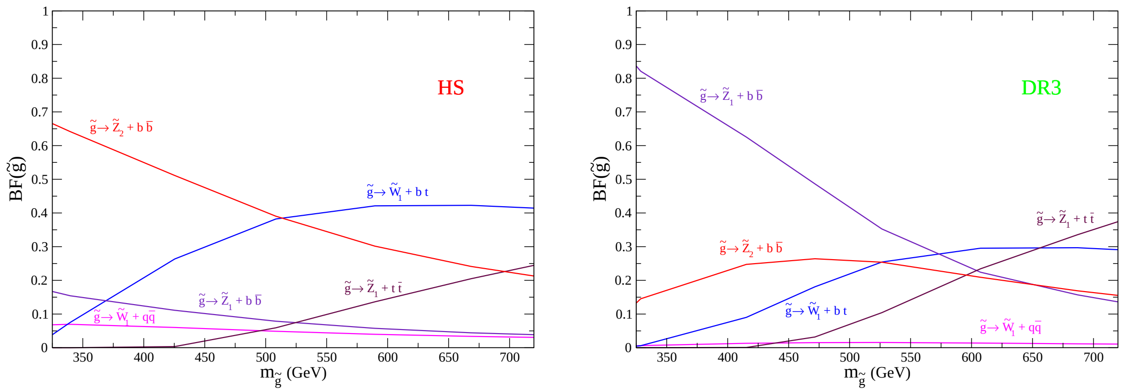

Figure 2: Gluino branching ratios for typical HS and DR3 model-lines as a function of the gluino mass.

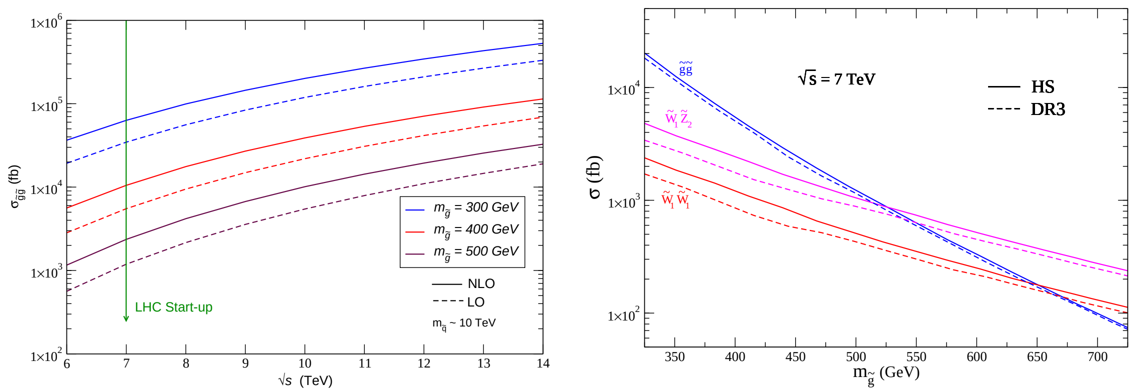

Figure 3: Left: Total cross-section for gluino pair production with $m_{\tilde q} = 10$ TeV versus LHC collider energy $\sqrt{s}$, for $m_{\tilde g} = 300$, 400 and 500 GeV. Right: Leading order total cross-sections for sparticle production in the HS and DR3 models as a function of the gluino mass for pp collisions at $\sqrt{s} = 7$ TeV.

Putting all segments of the cascade decays together, we expect the HS signal to be rich in b-jets and opposite-sign/same-flavor (OS/SF) isolated dileptons coming from $\widetilde Z_2 \to \widetilde Z_1 \ell\bar\ell$, and/or SS dileptons coming from $\tilde g \to \widetilde W_1 q\bar q'$ followed by $\widetilde W_1 \to \ell\nu_\ell \widetilde Z_1$ decay. For the DR3 point, we expect the signal to be rich in b-jets with a harder $E_T^{\rm miss}$ spectrum (when compared to the HS case) due to the direct gluino decay to $\widetilde Z_1$, at least for $m_{\tilde g} < 500$ GeV, but with small rates in the multilepton channels.

3 LHC discovery potential at 7 TeV

Let us now examine the discovery potential for Yukawa-unified SUSY, characterized by light gluinos, in the first phase of LHC operation. The left panel of Fig. 3 shows cross sections of gluino-pair production, $\sigma(pp \to \tilde g\tilde g X)$, as a function of the collider energy $\sqrt{s}$, for $m_{\tilde g} = 300$, 400 and 500 GeV, while taking $m_{\tilde q} = 10$ TeV. For $m_{\tilde g} = 400$ GeV, LHC operating at $\sqrt{s} = 7$ TeV yields a cross section of $\sigma \sim 10^4$ fb. It is expected that about 1 fb^{-1} of integrated luminosity will be collected at this energy. Then, the LHC should move up in energy, ultimately reaching its design energy of $\sqrt{s} = 14$ TeV, where the cross section increases to $\sim 10^5$ fb. The total cross-sections for sparticle production at $\sqrt{s} = 7$ TeV are shown in the right panel of Fig. 3.

In order to study the discovery potential of the LHC at $\sqrt{s} = 7$ TeV we used Isajet7.79 [27] to generate signal events for the HS and DR3 cases (the points HSb and DR3b mentioned below have $m_{\tilde g} \simeq 350$ GeV and $m_{\tilde g} \simeq 320$ GeV, respectively). Moreover, we used AlpGen [28] and MadGraph [29] to generate the background hard scattering events and Pythia [30] for the

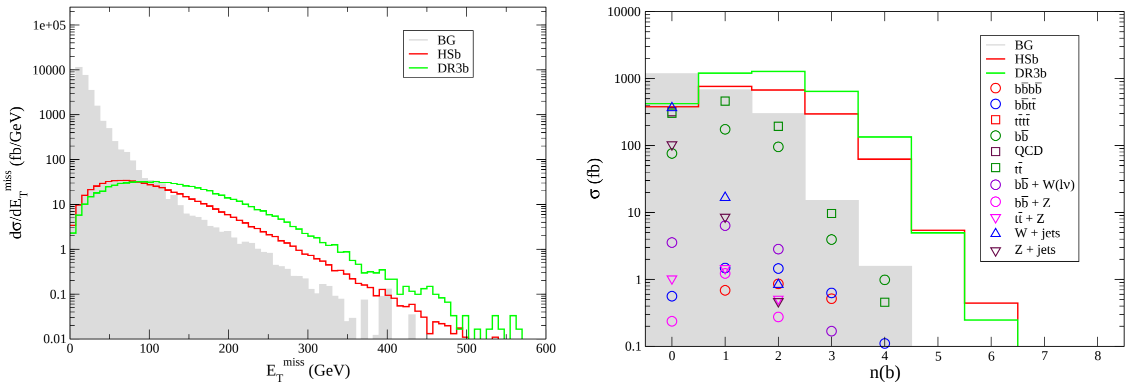

Figure 4: Signal (red/green lines for HSb/DR3b cases) and backgrounds (gray histograms) for Yukawa-unified SUSY at the LHC with $\sqrt{s} = 7$ TeV. Left: $E_T^{\rm miss}$ distribution after the C0 cuts. Right: b-jet distribution after adding a cut of $E_T^{\rm miss} > 100$ GeV (C1 cuts).

subsequent showering and hadronization.

A toy detector simulation is then employed with calorimeter cell size $\Delta\eta \times \Delta\phi = 0.05 \times 0.05$ and $-5 < \eta < 5$. The HCAL (hadronic calorimetry) energy resolution is taken to be $80\%/\sqrt{E} + 3\%$ for $|\eta| < 2.6$ and FCAL (forward calorimetry) is $100\%/\sqrt{E} + 5\%$ for $|\eta| > 2.6$, where the two terms are combined in quadrature. The ECAL (electromagnetic calorimetry) energy resolution is assumed to be $3\%/\sqrt{E} + 0.5\%$. We use the Isajet jet finding algorithm (cone type) to group the hadronic final states into jets. The jets and isolated lepton definitions are as follows: Jets are required to have $R \equiv \sqrt{\Delta\eta^2 + \Delta\phi^2} \leq 0.4$ and $E_T(jet) > 25$ GeV. Leptons are considered isolated if they have $p_T(l) > 5$ GeV with visible activity within a cone of $\Delta R < 0.2$ of $\Sigma E_T^{cells} < 5$ GeV.

Jets are tagged as b-jets if they contain a B hadron with $E_T(B) > 15$ GeV, $\eta(B) < 3$ and $\Delta R(B, jet) < 0.5$. We assume a tagging efficiency of 60% and light quark and gluon jets can be mis-tagged as a b-jet with a probability 1/150 for $E_T \leq 100$ GeV, 1/50 for $E_T \geq 250$ GeV, with a linear interpolation for 100 GeV $\leq E_T \leq$ 250 GeV. For more details, see [18].

Figure 4 (left panel) shows the $E_T^{\rm miss}$ distribution for signal and backgrounds (BG) after a basic set of cuts, which we call "C0 cuts":

- $n(jets) \geq 4$ with $E_T(j) \geq 50$ GeV, $\eta(j) \leq 3$ and for the hardest jet $E_T(j1) \geq 100$ GeV,
- $S_T \geq 0.2$,
- $n(b) \geq 1$,

where S_T is the transverse sphericity and $n(b)$ the number of b-jets. If no cut on $E_T^{\rm miss}$ is applied, the signal exceeds the BG for $n(b) \geq 4$. For both the HS and DR3 model lines, the approximate 5σ LHC reach extends to $m_{\tilde{g}} \sim 360$ GeV for 0.1 fb^{-1}, and ~ 400 GeV for 0.2 fb^{-1}. This is comparable to what Tevatron experiments can achieve using > 5 fb^{-1} of data (see below).

When a reliable $E_T^{\rm miss}$ measurement is available, supplementing the C0 cuts with a $E_T^{\rm miss} >$ 100 GeV requirement ("C1 cuts") leads to a drastic reduction of the BG. The $n(b)$ distribution after C1 cuts is shown in the right panel of Fig. 4. Now the signal's peak at $n(b)$ =1, 2 is visible above the BG, and the hard distribution in $n(b)$ should be a striking signature for both the DR3b and HSb models, since the combined signal plus BG distribution becomes approximately flat for $0 \leq n(b) \leq 2$. along with expected signal rates from the HS and DR3 model lines. Requiring $n(b) \geq 2$, we find an LHC reach for Yukawa-unifed SUSY out to $m_{\tilde{g}} = 500$ (600) GeV for 0.2 (1) fb^{-1}. For $n(b) \geq 3$, the SM background is greatly reduced. In this case, we find a reach to $m_{\tilde{g}} = 540$ (630) GeV for 0.2 (1) fb^{-1}. The reach is largely independent of whether one

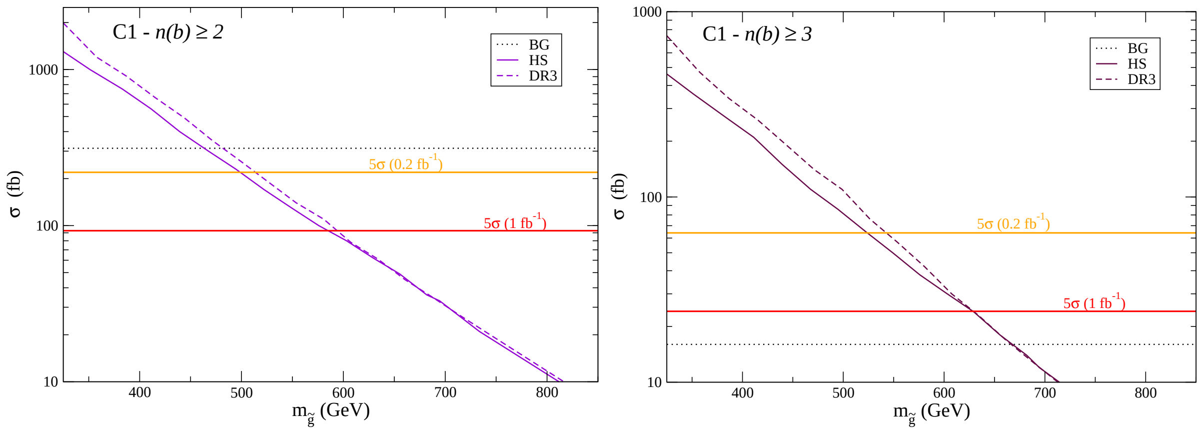

Figure 5: Early LHC reach for Yukawa-unified SUSY using cuts $C1$ plus $n_b \geq 2$ and $n_b \geq 3$.

is in the HS or the DR3 model. The SM background level and 5σ level for 0.2 and 1 fb^{-1} are shown in the plots of Fig. 5,

A corrorating signal should be observable in the OS/SF dilepton channel. For the HS model, where we obtain a high rate for $\tilde{g} \to b\bar{b}\widetilde{Z}_2$ decays, we find a reach up to $m_{\tilde{g}} = 400$ (500) GeV for 0.2 (1) fb^{-1} of integrated luminosity. For the DR3 model line, there is no reach for 0.2 fb^{-1}, since here the $\tilde{g} \to b\bar{b}\widetilde{Z}_1$ decay is dominant. With 1 fb^{-1}, however, a signal with 5σ significance should be visible for $m_{\tilde{g}} \sim 300 - 450$ GeV.

4 Competition from the Tevatron

The light gluinos in the mass range we are considering here are of course also searched for at the Fermilab Tevatron collider. While negative searches for gluino pair production currently require (under an analysis with ~ 2 fb^{-1} of integrated luminosity) $m_{\tilde{g}} \geq 308$ GeV [31,32] in mSUGRA-like models, use has not yet been made of the large gluino pair production cross section and high b-jet multiplicity expected from Yukawa unified models.

Indeed gluino-pair production cross sections at the Tevatron are greatly enhanced in Yukawa-unified scenarios. The reason is that the production is dominated by $q\bar{q} \to \tilde{g}\tilde{g}$, which receives contributions from s-channel gluon exchange, along with t- and u- channel squark exchange diagrams.The st- and su-channel interference terms contribute *negatively* to the total production cross section, thereby leading to an actual suppression of $\sigma(p\bar{p} \to \tilde{g}\tilde{g}X)$ for $m_{\tilde{q}} \sim m_{\tilde{g}}$. For $m_{\tilde{q}} \gg m_{\tilde{g}}$ on the other hand, the t-channel, u-channel and interference terms are all highly suppressed, leaving the s-channel gluon exchange contribution unsuppressed and dominant. The situation is illustrated in Fig. 6, where we plot the LO and NLO gluino pair production cross section for $m_{\tilde{g}} = 300$, 400 and 500 GeV versus $m_{\tilde{q}}$. We see that as $m_{\tilde{q}}$ grows, the total production cross section *increases*, and by a large factor: for $m_{\tilde{g}} = 400$ GeV, as $m_{\tilde{q}}$ varies from 400 GeV to 10 TeV, we see a factor of ~ 10 increase in total rate!

We again point out the importance of exploiting the b-jet multiplicity to maximize the discovery reach. By requiring Tevatron events with ≥ 4 jets plus large $E_T^{\rm miss}$, along with ≥ 2 or 3 tagged b-jets, QCD and electroweak backgrounds can be substantially reduced relative to expected signal rates. In [19] we found that the CDF and D0 experiments should be sensitive to $m_{\tilde{g}} \sim 400 - 440$ GeV with $5 - 10$ fb^{-1} of integrated luminosity. Thus, Tevatron experiments are sensitive to much higher values of gluino mass than otherwise expected from conventional searches. With $5 - 10$ fb^{-1} of data, Tevatron experiments can indeed begin to explore a large swath of Yukawa-unified SUSY model parameter space.

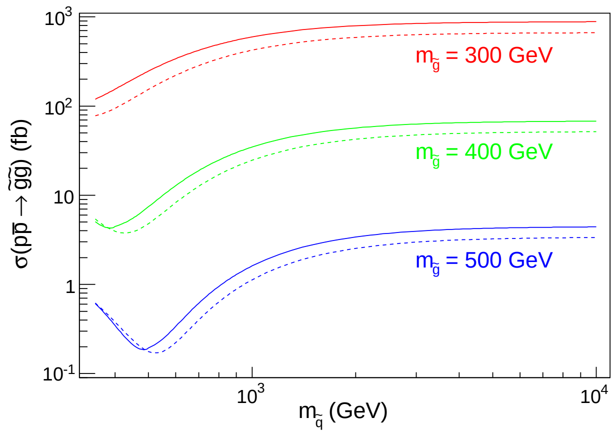

Figure 6: Cross section of gluino pair production (in fb) at the Fermilab Tevatron collider as a function of $m_{\tilde{q}}$, for $m_{\tilde{g}} = 300$, 400 and 500 GeV. Dashed is LO QCD, while solid is NLO, as given by Prospino.

5 Conclusions

In $t - b - \tau$ Yukawa-unified SUSY, we expect a characteristic spectrum of superpartners with first/second generation squarks and sleptons around 10 TeV, third generation sparticles, heavy Higgs bosons and μ around the few TeV level, and very light gauginos, with $m_{\tilde{g}} \sim 300 - 500$ GeV (although here we consider even higher values). Thus, at LHC, we expect to see gluino pair production at a high rate, followed by gluino decays to $b\bar{b}\widetilde{Z}_i$ or $t\bar{b}\widetilde{W}_1^- + c.c.$. SUSY searches should therefore exploit the high multiplicity of b-jets expected in this scenario.

The LHC reach at very low luminosity and without $E_T^{\rm miss}$, but requiring $n(b) \geq 4$, is about $m_{\tilde{g}} \sim 400$ GeV. This is comparable to the Tevatron reach in the multi-$b + E_T^{\rm miss}$ channel with 5–10 fb^{-1} of data. This may lead to a tight competition for the discovery or exclusion of the simplest Yukawa-unified SUSY scenario. When a reliable $E_T^{\rm miss}$ resolution is available, we find that the LHC reach, using $\sqrt{s} = 7$ TeV and 1 fb^{-1} of integrated luminosity, will move into the $m_{\tilde{g}} \sim 600 - 650$ GeV range for both the HS and DR3 model lines, if we require $E_T^{\rm miss} \geq 100$ GeV along with $n(b) \geq 3$.

Thus, our main conclusion is that at its first stage of operation theLHC stands an excellent chance to either discover Yukawa-unifed SUSY, or exclude almost all its model parameter space!

References

1. For recent reviews, see R. Mohapatra, hep-ph/9911272 and S. Raby, in *Rept. Prog. Phys.* 67 (2004) 755.
2. H. Georgi, in *Proceedings of the American Institue of Physics*, edited by C. Carlson (1974); H. Fritzsch and P. Minkowski, *Ann. Phys.* 93, 193 (1975); M. Gell-Mann, P. Ramond and R. Slansky, *Rev. Mod. Phys.* 50, 721 (1978).
3. P. Minkowski, *Phys. Lett.* B67 (1977) 421; M. Gell-Mann, P. Ramond and R. Slansky, in *Supergravity, Proceedings of the Workshop*, Stony Brook, NY 1979 (North-Holland, Amsterdam); T. Yanagida, KEK Report No. 79-18, 1979; R. Mohapatra and G. Senjanovic, *Phys. Rev. Lett.*44 (1980) 912.
4. B. Ananthanarayan, G. Lazarides and Q. Shafi, *Phys. Rev.* D44 (1991) 1613 and *Phys. Lett.* B300 (1993) 245; G. Anderson *et al.* *Phys. Rev.* D47 (1993) 3702 and *Phys. Rev.* D49 (1994) 3660; V. Barger, M. Berger and P. Ohmann, *Phys. Rev.* D49 (1994) 4908; M. Carena, M. Olechowski, S. Pokorski and C. Wagner, *Nucl. Phys.* B426 (1994) 269; B.

Ananthanarayan, Q. Shafi and X. Wang, *Phys. Rev.* D50 (1994) 5980; R. Rattazzi and U. Sarid, *Phys. Rev.* D53 (1996) 1553; T. Blazek, M. Carena, S. Raby and C. Wagner, *Phys. Rev.* D56 (1997) 6919; T. Blazek and S. Raby, *Phys. Lett.* B392 (1997) 371; T. Blazek and S. Raby, *Phys. Rev.* D59 (1999) 095002; T. Blazek, S. Raby and K. Tobe, *Phys. Rev.* D60 (1999) 113001 and *Phys. Rev.* D62 (2000) 055001.

5. S. Profumo, *Phys. Rev.* D68 (2003) 015006; C. Pallis, *Nucl. Phys.* B678 (2004) 398; M. Gomez, G. Lazarides and C. Pallis, *Phys. Rev.* D61 (2000) 123512, *Nucl. Phys.* B638 (2002) 165 and *Phys. Rev.* D67 (2003) 097701; U. Chattopadhyay, A. Corsetti and P. Nath, *Phys. Rev.* D66 (2002) 035003; M. Gomez, T. Ibrahim, P. Nath and S. Skadhauge, *Phys. Rev.* D72 (2005) 095008.
6. H. Baer, M. Diaz, J. Ferrandis and X. Tata, *Phys. Rev.* D61 (2000) 111701; H. Baer, M. Brhlik, M. Diaz, J. Ferrandis, P. Mercadante, P. Quintana and X. Tata, *Phys. Rev.* D63 (2001) 015007.
7. H. Baer and J. Ferrandis, *Phys. Rev. Lett.*87 (2001) 211803;
8. T. Blazek, R. Dermisek and S. Raby, *Phys. Rev. Lett.*88 (2002) 111804; T. Blazek, R. Dermisek and S. Raby, *Phys. Rev.* D65 (2002) 115004; R. Dermisek, S. Raby, L. Roszkowski and R. Ruiz de Austri, *JHEP* 0304 (2003) 037; R. Dermisek, S. Raby, L. Roszkowski and R. Ruiz de Austri, *JHEP* 0509 (2005) 029.
9. D. Auto, H. Baer, C. Balazs, A. Belyaev, J. Ferrandis, X. Tata, *JHEP* 0306 (2003) 023.
10. C. Balazs and R. Dermisek, *JHEP* 0803 (2003) 024.
11. H. Baer, S. Kraml, S. Sekmen and H. Summy, *JHEP* 0803 (2008) 056.
12. W. Altmannshofer, D. Guadagnoli, S. Raby and D. Straub, *Phys. Lett.* B668 (2008) 385.
13. I. Gogoladze, R. Khalid and Q. Shafi, *Phys. Rev.* D79 (2009) 115004.
14. D. Guadagnoli, S. Raby and D. M. Straub, *JHEP* 0910 (2009) 059.
15. H. Baer, S. Kraml and S. Sekmen, *JHEP* 0909 (2009) 005.
16. S. P. Martin and M. Vaughn, *Phys. Rev.* D50 (1994) 2282.
17. R. Hempfling, *Phys. Rev.* D49 (1994) 6168; L. J. Hall, R. Rattazzi and U. Sarid, *Phys. Rev.* D50 (1994) 7048; M. Carena *et al.*, *Nucl. Phys.* B426 (1994) 269; D. Pierce, J. Bagger, K. Matchev and R. Zhang, *Nucl. Phys.* B491 (1997) 3.
18. H. Baer, S. Kraml, A. Lessa, S. Sekmen and H. Summy, *JHEP* 1002 (2010) 055.
19. H. Baer, S. Kraml, A. Lessa, S. Sekmen and H. Summy, *Phys. Lett.* B685 (2010) 72.
20. R. Peccei and H. Quinn, *Phys. Rev. Lett.*38 (1977) 1440 and *Phys. Rev.* D16 (1977) 1791.
21. S. Weinberg, *Phys. Rev. Lett.*40 (1978) 223; F. Wilczek, *Phys. Rev. Lett.*40 (1978) 279.
22. J. E. Kim, *Phys. Rev. Lett.*43 (1979) 103; M. A. Shifman, A. Vainstein and V. I. Zakharov, *Nucl. Phys.* B166 (1980) 493.
23. M. Dine, W. Fischler and M. Srednicki, *Phys. Lett.* B104 (1981) 199; A. P. Zhitnitskii, *Sov. J. Nucl.* 31 (1980) 260.
24. For recent reviews, see J. E. Kim and G. Carosi, arXiv:0807.3125; P. Sikivie, *AIP Conf. Proc.* 805 (2006) 23, hep-ph/0509198; M. Turner, *Phys. Rept.* 197 (1990) 67.
25. H. P. Nilles and S. Raby, *Nucl. Phys.* B198 (1982) 102; J. E. Kim and H. P. Nilles, *Phys. Lett.* B138 (1984) 150; J. E. Kim, *Phys. Lett.* B136 (1984) 378.
26. H. Baer, M. Haider, S. Kraml, S. Sekmen and H. Summy, JCAP**0902** (2009) 002.
27. ISAJET v7.79, by H. Baer, F. Paige, S. Protopopescu and X. Tata, hep-ph/0312045.
28. M. Mangano, M. Moretti, F. Piccinini, R. Pittau and A. Polosa, *JHEP* 0307 (2003) 001.
29. T. Stelzer and W. F. Long, *Comput. Phys. Commun.* 81 (1994) 357.
30. T. Sjostrand, S. Mrenna and P. Skands, *JHEP* 0605 (2006) 026.
31. T. Aaltonen *et al.* (CDF Collaboration), *Phys. Rev. Lett.*102 (2009) 121801.
32. V. M. Abazov *et al.* (D0 Collaboration), *Phys. Lett.* B660 (2008) 449.